J|A|C|S ARTICLES

Published on Web 12/28/2009

Functionalization in Flexible Porous Solids: Effects on the Pore Opening and the Host−Guest Interactions

Thomas Devic,*,† Patricia Horcajada,† Christian Serre,† Fabrice Salles,‡ Guillaume Maurin,‡ Béatrice Moulin,§ Daniela Heurtaux,† Guillaume Clet,§ Alexandre Vimont,§ Jean-Marc Grenèche,|| Benjamin Le Ouay,† Florian Moreau,† Emmanuel Magnier,† Yaroslav Filinchuk,⊥ Jerôme Marrot,† Jean-Claude Lavalley,§ Marco Daturi,§ and Gérard Férey†

Institut Lavoisier, UMR CNRS 8180, Université de Versailles Saint-Quentin-en-Yvelines, 45 avenue des Etats-Unis, 78035 Versailles cedex, France, Institut Charles Gerhardt Montpellier, UMR CNRS 5253, UM2, ENSCM, Place E. Bataillon, 34095 Montpellier cedex 05 France, Laboratoire Catalyse et Spectrochimie, ENSICAEN, Université de Caen, CNRS, 6 Bd Maréchal Juin, 14050 Caen, France, Laboratoire de Physique de l'Etat Condensé, UMR CNRS 6087, Université du Maine, 72085 Le Mans Cedex, France, and Swiss-Norwegian Beamlines at ESRF, 38043 Grenoble, France

Received November 3, 2009; E-mail: devic@chimie.uvsq.fr

Abstract: The synthesis on the gram scale and characterization of a series of flexible functionalized iron terephthalate MIL-53(Fe) type solids are reported. Chemical groups of various polarities, hydrophilicities, and acidities (−Cl, −Br, $-CF_3$, $-CH_3$, $-NH_2$, −OH, $-CO_2H$) were introduced through the aromatic linker, to systematically modify the pore surface. X-ray powder diffraction (XRPD), molecular simulations, thermogravimetric analyses, and *in situ* IR and ^{57}Fe Mössbauer spectrometries indicate some similarities with the pristine MIL-53(Fe) solid, with the adoption of the *narrow pore* form for all solids in both the hydrated and dry forms. Combined XRPD and computational structure determinations allow concluding that the geometry of the pore opening is predominantly correlated with the intraframework interactions rather than the steric hindrance of the substituent. Only (MIL-53(Fe)-$(CF_3)_2$) exhibits a nitrogen accessible porosity ($S_{BET} \approx 100$ m^2 g^{-1}). The adsorption of some liquids leads to pore openings showing some very specific behaviors depending on the guest−MIL-53(Fe) framework interactions, which can be related to the energy difference between the *narrow* and *large pore* forms evaluated by molecular simulation.

Introduction

One method for modulating the storage/separation properties of hybrid Porous Coordination Polymers (PCPs) or Metal Organic Frameworks (MOFs)[1−3] is to functionalize the organic component of their walls with groups of variable polarities, acidities, etc., influencing the sorption and selectivity processes. The functionalization of *rigid* MOFs has been investigated, either starting simply from linkers containing halogen atoms, amine, amide, or alkyl groups[4−12] or by postsynthetic modifications,[13−26] with, in some cases, an evaluation of their resulting sorption properties[27,28] or catalytic activities.[29,30] On the contrary, only a few studies concern *flexible* MOFs.[31−34] In this case, the functionalization not only affects the nature of the pore surfaces, and thus the strength of the host−guest interactions, but also changes the flexible character (pore opening/closing, magnitude, etc.) and the adsorption properties in a more complex way. The present study concerns our series of flexible M^{III} hydroxo terephthalates denoted MIL-53(M) (M = Cr, Al, Fe, Ga, In; MIL = Materials of Institut Lavoisier) or (M^{III}(OH)-$(O_2C-C_6H_4-CO_2)$), which are three-dimensional porous solids built up from chains of corner-sharing $MO_4(OH)_2$ octahedra, connected through terephthalate linkers to define diamond-

† Institut Lavoisier.
‡ Institut Charles Gerhardt Montpellier.
§ Université de Caen.
|| Université du Maine.
⊥ Swiss Norvegian Beamlines at ESRF.

(1) Férey, G. *Chem. Soc. Rev.* **2008**, *37*, 191–214.
(2) Yaghi, O. M.; O'Keeffe, M.; Ockwig, N. W.; Chae, H. K.; Eddaoudi, M.; Kim, J. *Nature* **2003**, *423*, 705–714.
(3) Kitagawa, S.; Kitaura, R.; Noro, S.-I. *Angew. Chem., Int. Ed.* **2004**, *43*, 2334–2375.
(4) Braun, M. E.; Steffek, C. D.; Kim, J.; Rasmussen, P. G.; Yaghi, O. M. *Chem. Commun.* **2001**, 2532–2533.
(5) Custelcean, R.; Gorbunova, M. G. *J. Am. Chem. Soc.* **2005**, *127*, 16362–16363.
(6) Gadzikwa, T.; Zeng, B.-S.; Hupp, J. T.; Nguyen, S. T. *Chem. Commun.* **2008**, 3672–3674.
(7) Grzesiak, A. L.; Uribe, F. J.; Ockwig, N. W.; Yaghi, O. M.; Matzger, A. J. *Angew. Chem., Int. Ed.* **2006**, *45*, 2553–2556.
(8) Eddaoudi, M.; Kim, J.; Rosi, N.; Vodak, D.; Wachter, J.; O'Keeffe, M.; Yaghi, O. M. *Science* **2002**, *295*, 469–472.
(9) Yang, C.; Wang, X.; Omary, M. A. *J. Am. Chem. Soc.* **2007**, *129*, 15454–15455.
(10) Tanaka, D.; Masaoka, S.; Horike, S.; Furukawa, S.; Mizuno, M.; Endo, K.; Kitagawa, S. *Angew. Chem., Int. Ed.* **2006**, *45*, 4628–4631.
(11) Li, J.-R.; Tao, Y.; Yu, Q.; Bu, X.-H.; Sakamoto, H.; Kitagawa, S. *Chem.—Eur. J.* **2008**, *14*, 2771–2776.
(12) Horike, S.; Bureekaew, S.; Kitagawa, S. *Chem. Commun.* **2008**, 471–473.
(13) Burrows, A. D.; Frost, C. G.; Mahon, M. F.; Richardson, C. *Angew. Chem., Int. Ed.* **2008**, *47*, 8482–8486.

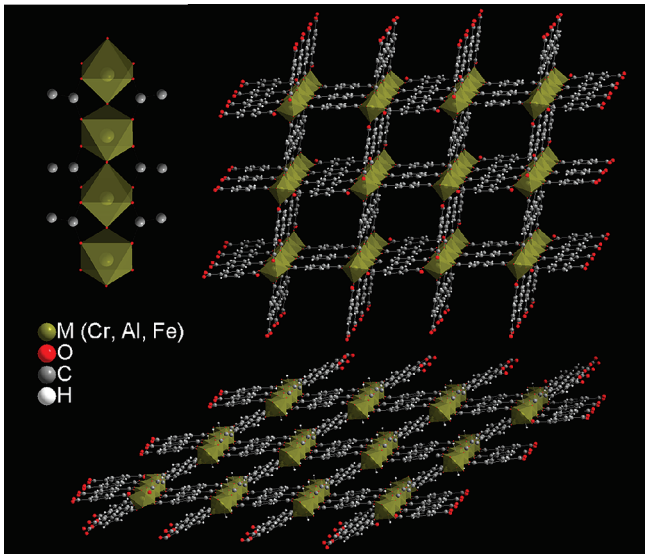

Figure 1. View of the structure of MIL-53(M). Left: chains of corner sharing $MO_4(OH)_2$ octahedra. Right: the 3-dimensional framework shown along the pores axis, in both its large pore (top) and narrow pore (bottom) form.

shaped one-dimensional channels (Figure 1).[35−38] This structure currently represents the archetype of flexible solids which, depending on both the nature of guests and the temperature, evolve from a *narrow pore (np)* to a *large pore (lp)* form (see Figure 1) with a variation of their cell volume (up to 40%) without any bond breaking.

The explored guests up to now are water,[35,36,39,40] carbon dioxide,[41,42] linear alkanes,[43−45] Ibuprofen,[46] xylenes,[47] or other liquids.[48−50] Moreover, the nature of the form strongly depends on the nature of the M^{III} metal, with a very different flexible character for the MIL-53(Fe) solid[37,46] compared with its Cr, Al, or Ga analogues.[39,51] While the Al, Cr dried solids possess a *large pore* structure at room temperature that might shrink or not upon adsorption,[41,43,44] the iron solid exhibits a close *narrow pore* dried form that turns into larger pore forms through two structural transitions upon adsorption of guest molecules.[39,45,48] MIL-53(Ga) exhibits an intermediate behavior with a *narrow pore* dried form at room temperature that further reopens at higher temperature.[51] It was shown that the *narrow pore* and the *large pore* forms are rather close in energy and that the host−guest interactions should overcome an energy barrier (∼20 kJ mol^{-1} for MIL-53(Cr)[40,43]) to switch from one form to the other.[42]

First attempts of functionalization have concerned a basic group (introduction of one $-NH_2$ per linker for MIL-53(Al, Fe),[32,52,53] acidic groups (introduction of one −OH or two $-CO_2H$ per linker in MIL-53(Al)[54] and (Fe)[55] respectively), and apolar groups (introduction of one phenyl or four $-CH_3$ groups per linker in MIL-53(Al)[56] and (Cr)[57] respectively). Polar

(14) Dugan, E.; Wang, Z.; Okamura, M.; Medina, A.; Cohen, S. M. *Chem. Commun.* **2008**, 3366–3368.
(15) Gadzikwa, T.; Lu, G.; Stern, C. L.; Wilson, S. R.; Hupp, J. T.; Nguyen, S. T. *Chem. Commun.* **2008**, 5493–5495.
(16) Goto, Y.; Sato, H.; Shinkai, S.; Sada, K. *J. Am. Chem. Soc.* **2008**, *130*, 14354–14355.
(17) Haneda, T.; Kawano, M.; Kawamichi, T.; Fujita, M. *J. Am. Chem. Soc.* **2008**, *130*, 1578–1579.
(18) Ingleson, M. J.; Barrio, J. P.; Guilbaud, J.-B.; Khimyak, Y. Z.; Rosseinsky, M. J. *Chem. Commun.* **2008**, 2680–2682.
(19) Kawamichi, T.; Kodama, T.; Kawano, M.; Fujita, M. *Angew. Chem., Int. Ed.* **2008**, *47*, 8030–8032.
(20) Kaye, S. S.; Long, J. R. *J. Am. Chem. Soc.* **2008**, *130*, 806–807.
(21) Morris, W.; Doonan, C. J.; Furukawa, H.; Banerjee, R.; Yaghi, O. M. *J. Am. Chem. Soc.* **2008**, *130*, 12626–12627.
(22) Tanabe, K. K.; Wang, Z.; Cohen, S. M. *J. Am. Chem. Soc.* **2008**, *130*, 8508–8517.
(23) Wang, Z.; Cohen, S. M. *J. Am. Chem. Soc.* **2007**, *129*, 12368–12369.
(24) Wang, Z.; Cohen, S. M. *Angew. Chem., Int. Ed.* **2008**, *47*, 4699–4702.
(25) Wang, Z.; Tanabe, K. K.; Cohen, S. M. *Inorg. Chem.* **2009**, *48*, 296–306.
(26) Meilikhov, M.; Yusenko, K.; Fischer, R. A. *J. Am. Chem. Soc.* **2009**, *131*, 9644–9645.
(27) Rowsell, J. L. C.; Millward, A. R.; Park, K. S.; Yaghi, O. M. *J. Am. Chem. Soc.* **2004**, *126*, 5666–5667.
(28) Rowsell, J. L. C.; Yaghi, O. M. *J. Am. Chem. Soc.* **2006**, *128*, 1304–1315.
(29) Seo, J. S.; Whang, D.; Lee, H.; Jun, S. I.; Oh, J.; Jeon, Y. J.; Kim, K. *Nature* **2000**, *404*, 982–986.
(30) Hasegawa, S.; Horike, S.; Matsuda, R.; Furukawa, S.; Mochizuki, K.; Kinoshita, Y.; Kitagawa, S. *J. Am. Chem. Soc.* **2007**, *129*, 2607–2614.
(31) Ghosh, S. K.; Bureekaew, S.; Kitagawa, S. *Angew. Chem., Int. Ed.* **2008**, *47*, 3403–3406.
(32) Gascon, J.; Aktay, U.; D., H.-A. M.; van Klink, G. P. M.; Kaptejin, F. *J. Catal.* **2009**, *261*, 75–87.
(33) Kasai, K.; Fujita, M. *Chem.—Eur. J.* **2007**, *13*, 3089–3105.
(34) Yang, C.; Wang, X.; Omary, M. A. *Angew. Chem., Int. Ed.* **2009**, *48*, 2500–2505.
(35) Loiseau, T.; Serre, C.; Huguenard, C.; Fink, G.; Taulelle, F.; Henry, M.; Bataille, T.; Férey, G. *Chem.—Eur. J.* **2004**, *10*, 1373–1382.
(36) Serre, C.; Millange, F.; Thouvenot, C.; Nogues, M.; Marsolier, G.; Louer, D.; Ferey, G. *J. Am. Chem. Soc.* **2002**, *124*, 13519–13526.
(37) Whitfield, T. R.; Wang, X.; Liu, L.; Jacobson, A. J. *Solid State Sci.* **2005**, *7*, 1096–1103.
(38) Anokhina, E. V.; Vougo-Zanda, M.; Wang, X.; Jacobson, A. J. *J. Am. Chem. Soc.* **2005**, *127*, 15000–15001.
(39) Millange, F.; Guillou, N.; Walton, R. I.; Grenèche, J.-M.; Margiolaki, I.; Ferey, G. *Chem. Commun.* **2008**, 4732–4734.
(40) Devautour-Vinot, S.; Maurin, G.; Henn, F.; Serre, C.; Devic, T.; Férey, G. *Chem. Commun.* **2009**, 2733–2735.
(41) Serre, C.; Bourrelly, S.; Vimont, A.; Ramsahye, N. A.; Maurin, G.; Llewellyn, P. L.; Daturi, M.; Filinchuk, Y.; Leynaud, O.; Barnes, P.; Férey, G. *Adv. Mater.* **2007**, *19*, 2246–2251.
(42) Salles, F.; Ghoufi, A.; Maurin, G.; Bell, R. G.; Mellot-Draznieks, C.; Férey, G. *Angew. Chem., Int. Ed.* **2008**, *47*, 8487–8491.
(43) Llewellyn, P. L.; Maurin, G.; Devic, T.; Loera-Serna, S.; Rosenbach, N.; Serre, C.; Bourrelly, S.; Horcajada, P.; Filinchuk, Y.; Férey, G. *J. Am. Chem. Soc.* **2008**, *130*, 12808–12814.
(44) Trung, T. K.; Trens, P.; Tanchoux, N.; Bourrelly, S.; Llewellyn, P. L.; Loera-Serna, S.; Serre, C.; Loiseau, T.; Fajula, F.; Férey, G. *J. Am. Chem. Soc.* **2008**, *130*, 16926–16932.
(45) Llewellyn, P. L.; Horcajada, P.; Maurin, G.; Devic, T.; Rosenbach, N.; Bourrelly, S.; Serre, C.; Vincent, D.; Loera-Serna, S.; Filinchuk, Y.; Férey, G. *J. Am. Chem. Soc.* **2009**, *131*, 13002–13008.
(46) Horcajada, P.; Serre, C.; Maurin, G.; Ramsahye, N. A.; Balas, F.; Vallet-Regi, M.; Sebban, M.; Taulelle, F.; Férey, G. *J. Am. Chem. Soc.* **2008**, *130*, 6774–6780.
(47) Alaerts, L.; Maes, M.; Giebeler, L.; Jacobs, P. A.; Martens, J. A.; Denayer, J. F. M.; Kirschhock, C. E. A.; De Vos, D. E. *J. Am. Chem. Soc.* **2008**, *130*, 14170–14178.
(48) Millange, F.; Serre, C.; Guillou, N.; Férey, G.; Walton, R. I. *Angew. Chem., Int. Ed.* **2008**, *47*, 4100–4105.
(49) Vougo-Zanda, M.; Huang, J.; Anokhina, E.; Wang, X.; Jacobson, A. J. *Inorg. Chem.* **2008**, *47*, 11535–11542.
(50) Wang, X. S.; Liu, L.; Jacobson, A. J. *Angew. Chem., Int. Ed.* **2006**, *45*, 6499–6503.
(51) Volkringer, C.; Loiseau, T.; Guillou, N.; Férey, G.; Elkaïm, E.; Vimont, A. *Dalton Trans.* **2009**, 2241–2249.
(52) Bauer, S.; Serre, C.; Devic, T.; Horcajada, P.; Marrot, J.; Férey, G.; Stock, N. *Inorg. Chem.* **2008**, *47*, 7568–7576.
(53) Couck, S.; Denayer, J. F. M.; Baron, G. V.; Rémy, T.; Gascon, J.; Kapteijn, F. *J. Am. Chem. Soc.* **2009**, *131*, 6326–6327.
(54) Himsl, D.; Wallacher, D.; Hartmann, M. *Angew. Chem., Int. Ed.* **2009**, *48*, 4639–4642.
(55) Sanselme, M.; Grenèche, J.-M.; Riou-Cavellec, M.; Férey, G. *Solid State Sci.* **2004**, *6*, 853–858.
(56) Comotti, A.; Bracco, S.; Sozzani, P.; Horike, S.; Matsuda, R.; Chen, J.; Takata, M.; Kubota, Y.; Kitagawa, S. *J. Am. Chem. Soc.* **2008**, *130*, 13664–13672.
(57) Serre, C.; Millange, F.; Devic, T.; Audebrand, N.; van Beek, W. *Mater. Res. Bull.* **2006**, *41*, 1550–1557.

Table 1. Synthesis Conditions of the MIL-53(Fe)-X_n Solids (X-Functionalized on the Phenyl Ring)[a]

Solid	Linker (mmol)	Iron(III) salt (mmol)	Solvent + HF 5 M (mL)	Synthesis	Guest exchange	Activation
MIL-53(Fe)-Cl[b]	$C_6H_3O_4Cl$ (1)[c]	Fe chloride (1)	DMF (5) + HF (1)	Autoclave (150 °C, 48 h)	No	−
MIL-53(Fe)-Cl	$C_6H_3O_4Cl$ (31)[c]	Fe chloride (31)	Water (300)	Reflux, 48 h	DMF (100 °C, 24 h)	150 °C, 80 h
MIL-53(Fe)-Br	$C_6H_3O_4Br$ (31)	Fe chloride (31)	Water (300)	Reflux, 48 h	DMF (100 °C, 24 h)	150 °C, 80 h
MIL-53(Fe)-CH_3	$C_6H_3O_4CH_3$ (10)[c]	Fe perchlorate (10)	DMF (50) + HF (1)	Autoclave (150 °C, 24 h)	No	200 °C, 72 h
MIL-53(Fe)-NH_2	$C_6H_3O_4NH_2$ (5)	Fe chloride (5)	Water (50)	Autoclave (150 °C, 72 h)	Ethanol (150 °C, 48 h)	150 °C, 72 h
MIL-53(Fe)-$(OH)_2$[b]	$C_6H_2O_4(OH)_2$ (6.8)[c]	Fe perchlorate (4.6)	DMF (25) + HF (1)	Autoclave (100 °C, 16 h)	No	150 °C, 15 h
MIL-53(Fe)-$(COOH)_2$	$C_6H_2O_4(COOH)_2$ (10)	Fe perchlorate (10)	Water (50)	Autoclave (150 °C, 16 h)	No	−
MIL-53(Fe)-$(CF_3)_2$	$C_6H_2O_4(CF_3)_2$ (2.5)[c]	Fe chloride (2.5)	Water (25)	Microwave (100 °C, 20 min)	No	250 °C, 48 h

[a] The general formula of these solids is $[Fe(OH)(C_6H_{4-n}O_4X_n)]\cdot G$ (G: guest). [b] These syntheses provided single crystals of the as-synthesized solids. [c] These ligands were prepared according to the procedure reported in the Supporting Information.

Scheme 1. Modified Terephthalate Linkers BDC-X_n Used in the Present Study

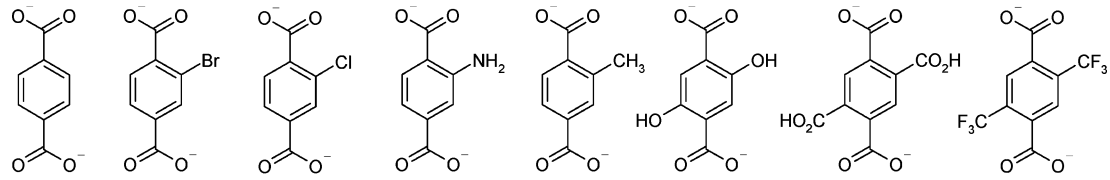

groups first led to enhanced properties in terms of gas separation (CO_2/CH_4),[53] adsorption capacity (H_2),[54] or basic catalysis,[32] whereas apolar groups emphasized the influence of the steric hindrance of the groups grafted onto the phenyl ring on the porosity of the material.[56,57] In MIL-53(Cr)-$(CH_3)_4$, it induces a rotation of the phenyl rings by 90°, which further prevents any adsorption of guests.[57]

Therefore, this paper aims at producing a large series of MIL-53(Fe)-X_n functionalized solids (X_n = −Cl, −Br, $-CH_3$, $-(CF_3)_2$, $-NH_2$, $-(OH)_2$, or $-(CO_2H)_2$) presenting a wide range of pore surface polarity, hydrophilicity, and acidity, to deeply evaluate by X-ray diffraction, *in situ* IR spectroscopy, TG analyses, and ^{57}Fe Mössbauer spectrometry the effect of such organic modifications both on the surface properties and on the breathing phenomenon. Moreover, plausible structural models for the different modified MIL-53(Fe) solids in the dry state and in the presence of solvent molecules have also been proposed by means of a computational structure determination starting with the lattice parameters obtained from the refinement of the experimental X-ray powder diffraction patterns (XRPD).

The first part of the paper is devoted to the characterization and analysis of various parameters of the hydrated MIL-53(Fe)-X_n solids, and the second to the dry ones. The effect of external stimuli (here adsorption of various liquids) on the flexible character of the functionalized MIL-53(Fe) solids is explored in the third part. Finally, the impact of the functionalization on the energetics of the *narrow pore−large pore* transition is discussed in light of the energy difference between the two structural forms simulated for each grafted group.

Experimental Section

Syntheses. Table 1 summarizes the main characteristics of the synthesis conditions which are described in detail in the Supporting Information. Two solids, namely MIL-53(Fe)-(NH_2)[52] and MIL-53(Fe)-$(CO_2H)_2$[55] (previously labeled MIL-82), were already described, but their preparation required the use of hydrofluoric acid. The present procedure is an HF-free alternative preparation. For the adsorption of liquids by functionalized MIL-53(Fe) solids, their activated forms were left in air for a few days, leading to their hydrated form. 10 to 40 mg of these solids were poured into 5 mL of a certain solvent (water, absolute ethanol, pyridine, and tetrachloroethane) and stirred for 24 h at room temperature. Small fractions of the resulting slurries were thus transferred into 1 mm glass capillaries, which were further sealed and left to stand for 5 days before an X-ray data collection.

Characterizations. The Supporting Information contains the details of the different techniques (single crystal and powder X-ray diffraction, thermal analyses (TGA, thermodiffractometry), and infrared and ^{57}Fe Mössbauer spectrometries) used for the characterization of the solids described in this article, as well as details of the molecular simulations.

Results and Discussion

In addition to their different steric hindrances, the selected terephthalic acid derivatives cover a broad spectrum of polarity, hydrophilicity, and acidity (Scheme 1).

Some Remarks on the As-Synthesized Solids. Their optimized syntheses allow us to obtain them at the 1−2 g scale, or even larger (10 g) for MIL-53(Fe)-X (X = Cl, Br) (see Figures S1 and S2-A for XRPD and IR characteristics of the as-synthesized solids). However, depending on the synthesis conditions (mainly the nature of the solvent, but not exclusively), the guests are different (H_2O, DMF, or even terephthalic acid). They can therefore induce specific and additional interactions with the framework, which partially conceals the inherent effect of functionalization on the breathing. This is the reason why, after their guest exchange and activation, all the solids were exposed to air for rehydratation, providing a homogeneous series with the same guest, suitable for establishing the effects of func-

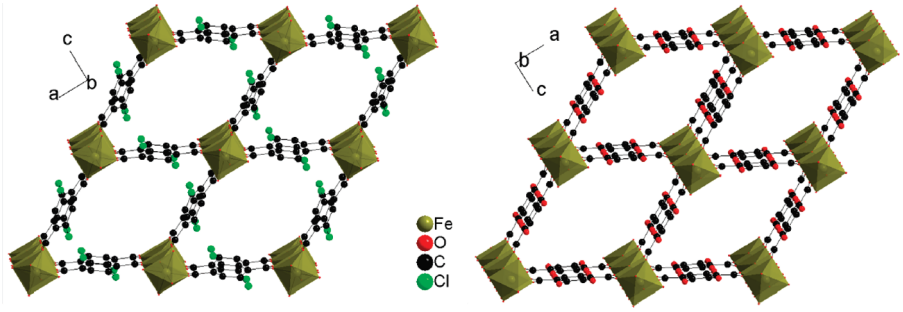

Figure 2. Single X-ray crystal structures of the as-synthesized MIL-53(Fe)-Cl (left) and MIL-53(Fe)-$(OH)_2$ (right) solids. Pore content was discarded during the refinement using the SQUEEZE procedure.

tionalization on their flexibility. IR spectra confirm the elimination of most of the free terephthalic acid and DMF molecules and the presence of adsorbed water in the rehydrated solid (Figure S2-B).

The information on the as-synthesized solids comes from the single crystal X-ray diffraction study of (MIL-53(Fe)-$(OH)_2$ and MIL-53(Fe)-Cl) (see Tables 1 and S1). Their structural characteristics (bond distances, etc.) are quasi-invariant (Figure 2), with the only difference being in the position of the phenyl rings. Indeed, in the case of the BDC-$(OH)_2$ linker, the phenyl ring lies parallel to the axis of the tunnels with the hydroxo groups statistically disordered over the 2 + 2 available positions on the phenyl ring. For the BDC-Cl derivative, a similar positional disorder is observed, but associated with an ~20° tilt of the phenyl ring relative to the pore axis, indicating an influence of the steric hindrance between the adjacent linkers.

Hydrated Forms of MIL-53(Fe)-X_n. The unit cells of the (air) hydrated functionalized MIL-53(Fe) solids were determined by XRPD. They are reported in Table 2 which gathers the crystallographic data on the dry, hydrated, and different post-solvated forms of the MIL-53(Fe)-X_n solids. All the hydrated solids exhibit the *narrow pore* form[35,36,39] with a monoclinic unit cell (space group *C*2/*c* (n°15)) and parameters very similar to those determined for the pristine hydrated MIL-53(M) (M = Cr, Al, Fe) solids. The slight variations of the parameters with $-(X)_n$ relate to the size and number of functional groups per iron and to the magnitude of the rotation of the phenyl ring, which will be discussed in the part devoted to the dry forms of the functionalized MIL-53(Fe) solids. It is worth noting that, whereas all the cell volumes are close to 1000 Å^3, X = CF_3 is an exception ($V \approx 1300$ Å^3), probably due to the huge steric hindrance of the CF_3 group. Indeed, in the case of MIL-53(Fe)-$(CF_3)_2$, a mixture of two forms (two pore openings) was observed. Once it was verified by IR spectroscopy as well as chemical and TG analyses that the guest was only water, this phenomenon was attributed to either a very slow adsorption of water after activation (as a consequence of the high hydrophobicity of the $-CF_3$ groups) or the coexistence of two phases, corresponding to different arrangements of the terephthalate cores as a result of different $-CF_3/-CF_3$ steric repulsion along the chain axis, giving rise to two pore openings (see Figure S8). Nevertheless, our computations show that two different arrangements of the $-CF_3$ groups considered initially in the *large pore* form lead to energy minimized structures with pore openings which differ by only 0.3 Å, a difference significantly weaker than the one observed experimentally. The first hypothesis (slow hydration) might therefore be the most realistic.

IR spectroscopy performed on the activated and rehydrated under air MIL-53(Fe)-$(X)_n$ (X = Cl, Br, CH_3, NH_2, CO_2H, CF_3) solids first indicates that the adsorbed water molecules can be easily eliminated. Upon outgassing at room temperature, the band associated with the adsorbed water ($\delta(H_2O) \approx 1620$ cm^{-1}) disappears, while those related to the bridging hydroxyl group (Fe−O(H)−Fe) ((ν(OH) and δ(OH) modes at approximately 3640 and 850 cm^{-1} respectively) become more resolved. In the hydrated form, these bands are broader and are located at approximately 3300 and 1050 cm^{-1} (Figure 3) due to weak hydrogen bonds between the water molecules and the bridging hydroxyl groups of the skeleton, as already observed for the MIL-53(Ga, Al) solids.[51]

All solids are stable up to 200 °C under vacuum, except MIL-53(Fe)-$(OH)_2$, as indicated by IR spectroscopy (see Figure S4). At a higher temperature (250 °C), destabilization of the structures begins, as evidenced from the decrease in intensity of the ν(OH) and δ(OH) bands of the hydroxyl groups in conjunction with a broadening of some terephthalate bands (1600 and 1150 cm^{-1}), corresponding to both a dehydroxylation and an amorphization of the structure. In the case of MIL-53(Fe)-$(OH)_2$, the amorphization starts at lower temperatures (150−200 °C) (Figure S4), a phenomenon that could be related to the redox reactivity of the 1,4-dihydroxyterephthalate.[58]

Further, the thermogravimetric analyses are consistent with the IR observations. All solids except MIL-53(Fe)-$(OH)_2$ exhibit a similar behavior (Figure S5), with the first weight loss at low temperature (T < 100 °C) associated with the water's departure and the second one at higher temperature associated with the collapse of the framework. This alteration of the solid takes place at 150−160 °C for MIL-53(Fe)-$(OH)_2$ and in the range 250−300 °C (lower than the nonfunctionalized MIL-53(Fe) (300−320 °C)) for the other solids. The residue corresponds to a poorly crystallized Fe_2O_3. The resulting weight losses (see Table S2) are consistent both with the chemical formulation Fe(OH)(BDC-X_n) and with the presence of roughly one water molecule per formula unit in the tunnels (except for MIL-53(Fe)-$(CF_3)_2$, see below), as for the pristine MIL-53(M) materials.

Finally, the removal of free water is surprisingly easier for most of the functionalized frameworks (100 °C or less) compared with the pristine solid (150 °C). This behavior shows that the introduction of functional groups does not lead to a drastic change of stability or large activation barriers which would otherwise prevent their use for gas sorption/separation applications. In the case of MIL-53(Fe)-$(OH)_2$, the difference between the first and second weight loss is less pronounced and may indicate that the collapse of the structure takes place before the complete dehydration (see below).

(58) Costentin, C.; Robert, M.; Saveant, J. M. *J. Am. Chem. Soc.* **2006**, *128*, 8726–8727.

Table 2. Unit-Cell Dimensions of the Functionalized MIL-53(Fe) Solids with Various Pore Fillings Determined from X-ray Powder Diffraction (* Corresponds to Mixtures of Narrow Pore and Large Pore Forms)

Solvent	S.G.	*a* (Å)	*b* (Å)	*c* (Å)	β (deg)	*V* (Å^3)
MIL-53(Fe)						
dry[39]	*C*2/*c*	21.269(1)	6.759(1)	6.884(1)	114.62(1)	899.6(1)
hydrated (air)[39]	*C*2/*c*	19.320(1)	2 × 7.518(1)	6.835(1)	96.305(1)	2 × 986.8(1)
water (liquid)[48]	*C*2/*c*	21.119(2)	7.664(1)	6.830(1)	114.87(1)	1003.0(2)
ethanol[48]	*Imcm*	16.183(2)	14.204(2)	6.895(1)	–	1584.9(3)
pyridine[48]	*C*2/*c*	19.196(2)	11.161(1)	6.885(1)	108.92(1)	1395.4(2)
tetrachloroethane	$P2_1/m$	18.739(3)	9.320(2)	7.050(1)	92.68(1)	1217.0(2)
MIL-53(Fe)-Cl						
dry	*C*2/*c*	20.112(4)	7.424(2)	6.898(2)	105.89(1)	990.5(4)
hydrated (air)	*C*2/*c*	20.116(2)	7.668(1)	6.859(1)	106.00(1)	1017.0(2)
water (liquid)	*C*2/*c*	20.094(3)	7.684(1)	6.853(1)	106.00(1)	1017.1(2)
ethanol	*Imcm*	16.819(1)	13.371(1)	6.913(1)	–	1554.7(2)
pyridine	*C*2/*c*	19.301(1)	11.169(1)	6.931(1)	108.99(1)	1412.8(1)
tetrachloroethane	*Imcm*	16.673(3)	13.509(2)	6.946(1)	–	1564.6(5)
MIL-53(Fe)-Br						
dry	*C*2/*c*	20.164(1)	7.996(1)	6.914(1)	106.95(1)	1066.3(1)
hydrated (air)	*C*2/*c*	20.227(1)	7.832(1)	6.906(1)	106.62(1)	1048.2(1)
water (liquid)	*C*2/*c*	20.254(1)	7.897(1)	6.912(1)	106.84(1)	1058.1(1)
ethanol	*Imcm*	16.711(1)	13.575(1)	6.923(1)	–	1570.4(1)
pyridine	*C*2/*c*	19.238(1)	11.245(1)	6.941(1)	108.75(1)	1421.9(1)
tetrachloroethane	*Imcm*	16.288(1)	13.721(1)	6.886(1)	–	1539.0(1)
MIL-53(Fe)-CH_3						
dry	*C*2/*c*	20.059(3)	7.947(2)	6.897(1)	106.43(1)	1054.6(3)
hydrated (air)	*C*2/*c*	20.075(2)	7.913(1)	6.887(1)	106.21(1)	1050.7(2)
water (liquid)	*C*2/*c*	20.078(1)	7.957(1)	6.890(1)	106.29(1)	1056.6(3)
ethanol	*Imcm*	16.627(1)	13.620(1)	6.929(1)	–	1569.1(2)
pyridine	*C*2/*c*	19.168(1)	11.372(1)	6.911(1)	19.49(1)	1440.2(1)
tetrachloroethane	*C*2/*c*	20.082(3)	7.903(1)	6.880(1)	106.28(1)	1048.2(2)
MIL-53(Fe)-NH_2						
dry	*C*2/*c*	20.148(1)	7.901(1)	6.978(1)	106.52(1)	1065.1(1)
hydrated (air)	*C*2/*c*	19.993(1)	7.724(1)	6.848(1)	105.32(1)	1019.9(1)
water (liquid)	*C*2/*c*	20.003(1)	7.737(1)	6.847(1)	105.38(1)	1021.7(1)
ethanol*	*C*2/*c*	20.029(2)	7.747(1)	6.860(1)	105.52(1)	1025.7(1)
	Imcm	16.323(2)	13.998(1)	6.903(1)	–	1577.2(3)
pyridine	*C*2/*c*	19.219(1)	11.157(1)	6.909(1)	108.73(1)	1403.0(1)
tetrachloroethane	*C*2/*c*	20.124(1)	7.913(5)	6.930(4)	106.64(3)	1057.0(1)
MIL-53(Fe)-$(OH)_2$						
dry[a]	*C*2/*c*	21.3	6.9	6.9	115	917
hydrated (air)	*C*2/*c*	19.909(2)	9.123(1)	6.832(1)	107.17(1)	1185.5(2)
water (liquid)	*Imcm*	17.368(1)	12.707(5)	6.891(1)	–	1520.7(1)
ethanol	*Imcm*	16.148(1)	14.404(1)	6.892(1)	–	1603.1(1)
pyridine	*C*2/*c*	19.924(3)	9.138(1)	6.827(1)	107.11(1)	1187.9(3)
tetrachloroethane*	*C*2/*c*	20.078(1)	9.010(1)	6.858(1)	107.15(1)	1185.5(2)
	Imcm	16.275(1)	13.947(2)	6.889(1)	–	1563.8(4)
MIL-53(Fe)-$(CO_2H)_2$						
dry	*C*2/*c*	20.013(1)	8.069(1)	6.967(1)	106.40(1)	1079.5(1)
hydrated (air)	*C*2/*c*	20.302(3)	8.116(1)	6.955(1)	107.32(1)	1094.1(3)
water (liquid)	*C*2/*c*	20.318(1)	8.123(1)	6.960(1)	107.34(2)	1096.5(1)
ethanol	*C*2/*c*	20.321(1)	8.125(1)	6.963(2)	107.34(1)	1097.3(1)
pyridine	*C*2/*c*	20.306(1)	8.120(1)	6.956(3)	107.33(2)	1094.9(1)
tetrachloroethane	*C*2/*c*	20.307(1)	8.117(1)	6.957(1)	107.32(1)	1094.6(1)
MIL-53(Fe)-$(CF_3)_2$						
dry*	*C*2/*c*	19.429(1)	10.355(1)	6.911(1)	108.57(1)	1317.9(1)
	Imcm	16.490(1)	13.653(2)	6.883(1)	–	1549.5(3)
hydrated (air)*	*C*2/*c*	19.425(2)	10.408(1)	6.905(1)	109.1(1)	1319.5(2)
water (liquid)*	*C*2/*c*	19.462(2)	10.341(1)	6.913(1)	108.53(1)	1319.2(2)
	Imcm	16.49 (1)	13.623(6)	6.882(2)	–	1546(4)
ethanol	*Imcm*	16.746(1)	13.605(1)	6.929(1)	–	1578.6(2)
pyridine	*Imcm*	15.917(2)	14.704(2)	6.933(1)	–	1622.5(3)
tetrachloroethane	*Imcm*	16.455(1)	13.793(1)	6.915(1)	–	1569.5(2)

[a] Estimated from thermodiffraction.

A typical X-ray thermodiffractogram of a modified MIL-53(Fe) solid is illustrated in Figure 4 (here MIL-53(Fe)-Br, see Figures S6 and S7 for the other solids). The Bragg peaks associated with the hydrated solids first slightly shift upon heating, as a consequence of both the departure of the water and the thermal expansion,[59] and finally vanish above 220 °C (−X = −OH), 260 °C (−X = −NH_2), or 300 °C (−X = −CH_3, −Br, −Cl, −CF_3 and −CO_2H). The latter change indicates the destruction of the hybrid frameworks, in agreement with the conclusions drawn from the IR and TG analyses.

Noteworthy, at variance to the pristine MIL-53(Fe) solid,[39,40] is the fact that no intermediate hemihydrated form is observed

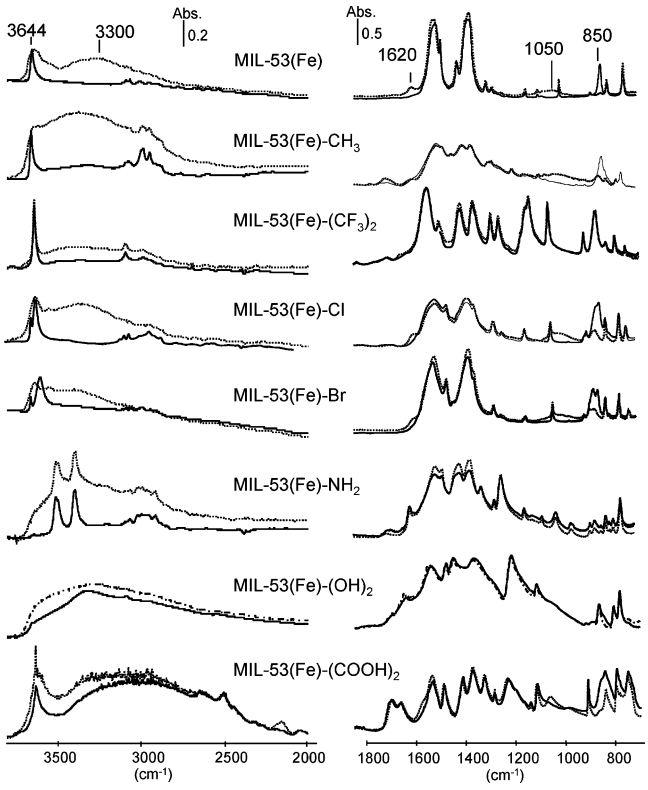

Figure 3. FTIR spectra of the activated functionalized MIL-53(Fe) solids. Dotted line: hydrated forms under air. Full line: dry forms outgassed at 423 K (MIL-53(Fe)-$(OH)_2$) or 473 K (MIL-53(Fe), MIL-53(Fe)-CH_3, MIL-53(Fe)-Br, MIL-53(Fe)-Cl, MIL-53(Fe)-$(CF_3)_2$, and MIL-53(Fe)-$(COOH)_2$).

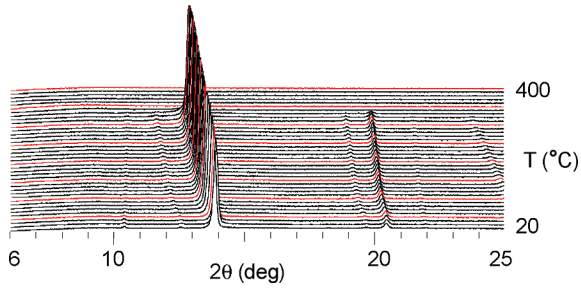

Figure 4. X-ray thermodiffractogram of the MIL-53(Fe)-Br solid performed under air (Co Kα, $\lambda \approx 1.7906$ Å).

in the series. Incidentally, we previously showed[39,55] that, for Fe(III)-containing hybrid porous solids, the presence of water in the pores influences the characteristics of the Mössbauer spectra. A similar study was therefore undertaken for the investigated series. Figure 5 illustrates the Mössbauer spectra recorded at 300 K and ambient pressure with a small velocity range to improve the resolution of the hyperfine structure. All the resulting spectra recorded at 77 K are rather similar. While, in all the structures described here, the Fe^{III} ions are on a single crystallographic site, the quadrupolar structure always consists of two main quadrupolar doublets, except that of MIL-53(Fe)-$(COOH)_2$ which seems to exhibit a single quadrupolar component. The isomer shift values are consistent with both the presence of only octahedral high spin Fe^{3+} sites and the absence of dense inorganic impurities such as iron oxide/hydroxides. Under vacuum at 300 K, all spectra exhibit a significant decrease of the outer quadrupolar component. Unfortunately, there is no clear quantitative correlation between the ratio of the intensities of each quadrupolar components and the nature of the substituent. Nevertheless, these results show that the perturbation on the iron site not only depends on the hydration state (as already observed in the nonmodified MIL-53(Fe)[39]) but also on the local perturbation in the environment of the iron(III) ion induced by the presence of substituents on the organic part.

Dry Forms of MIL-53(Fe)-X_n. The cell parameters of the dry forms of MIL-53(Fe)-X_n (X = Cl, Br, CH_3, NH_2, CO_2H, CF_3) were extracted from synchrotron XRPD at 303 K (see Table 2). The lower stability of MIL-53(Fe)-$(OH)_2$ prevented its isolation in the dry state, and the cell parameters were thus estimated from the thermodiffraction data. All solids exhibit comparable monoclinic unit cells (space group *C*2/*c*, a = 19.42−21.3 Å, b = 6.9−10.3 Å, c = 6.83−6.98 Å, β = 105.8°−115°), similar to those observed for the nonmodified solid.[39] These cell parameters therefore correspond to the ones of the *narrow pore* form, in agreement with the absence of any significant permanent porosity (Table S4). MIL-53(Fe)-CF_3, despite its large cell volume and noticeable BET surface area (96 $m^2\ g^{-1}$), which is largely determined by the steric hindrance of the CF_3 group, corresponds also to a *narrow pore* form (i.e., noticeably contracted compared to an orthorhombic *large pore* form). This behavior is also supported by our modeling approach, which shows that when the unit cell parameters of the *large pore* form of MIL-53(Fe)-$(CF_3)_2$ are fully relaxed, one obtains a final structure with a unit cell volume of 1283 $Å^3$ close to the experimental one, while, for the other modified structures, the same procedure leads to optimized structures with unit cell volumes ranging from 835 to 1213 $Å^3$, similar to the ones experimentally observed. Furthermore, starting from the experimental parameters, a plausible structural model for each dry functionalized-MIL-53(Fe) (Crystallographic Information Files provided in the Supporting Information) was built up using our computational approach described in the Supporting Information.

As stated in the introduction for MIL-53(Cr)-$(CH_3)_4$ (or MIL-105) with the same topology, the functionalization of the phenyl rings (hereafter noted Φ) can induce rotations of the rings (noted θ in Figure 6) with regard to the axis of the octahedral chains.[57] They can reach 90°, *a priori* depending on the number, the nature, and the steric hindrance of the substituent. Figure 6, related to the dry forms, illustrates that, in all the cells, the Φ rings are rotated (range 15°−35° depending on the nature of −X) with respect to the axis of the tunnels. The same feature occurs with the *large pore* forms, which exhibit different values for the angle of rotation (see Supporting Information). This implies that the host−guest interactions play a role in determining the dynamics of the structure. This calls for a reexamination of the effects of the functionalization on the rotations which occur around the Φ rings.

The first concerns the carboxylate function, which represents the linking part between the Φ rings and the inorganic chains Fe−OH−Fe. In terms of geometry, the COO group can rotate with respect to Φ. This rotation depends on the specific steric hindrance of the function grafted onto Φ and not directly on its volume, to take into account the anisotropy of the shape of the substituent. The larger the hindrance, the larger the γ angle between the COO group and Φ (Figure 7b).

This rotation immediately influences the tilting of the Fe octahedra around the Fe−Fe axis since each oxygen of the

(59) Barthelet, K.; Marrot, J.; Riou, D.; Férey, G. *Angew. Chem., Int. Ed.* **2002**, *41*, 281–284.

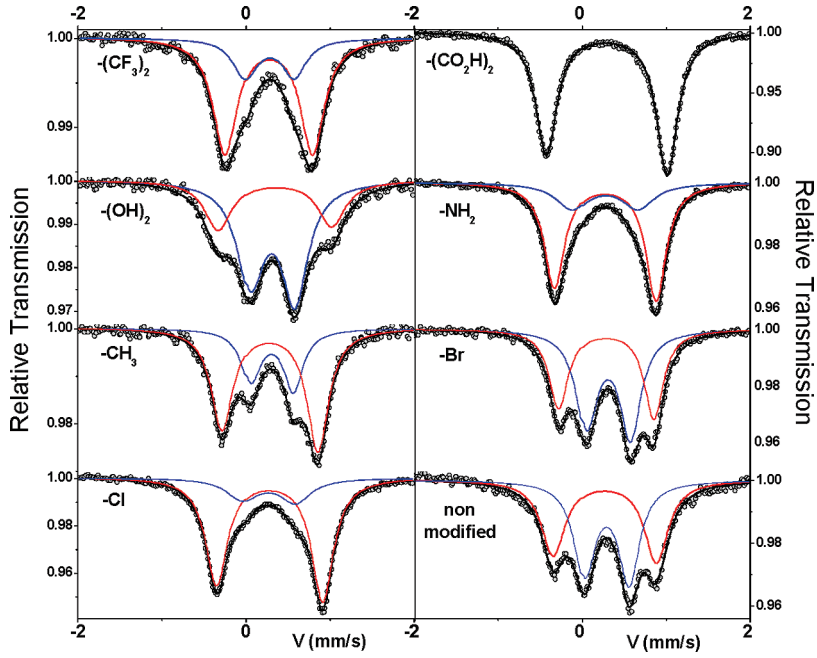

Figure 5. Mössbauer spectra of the modified MIL-53(Fe) solids (hydrated form) recorded at 300 K under air. They are compared to the one of the nonmodified MIL-53(Fe) solid (bottom right).

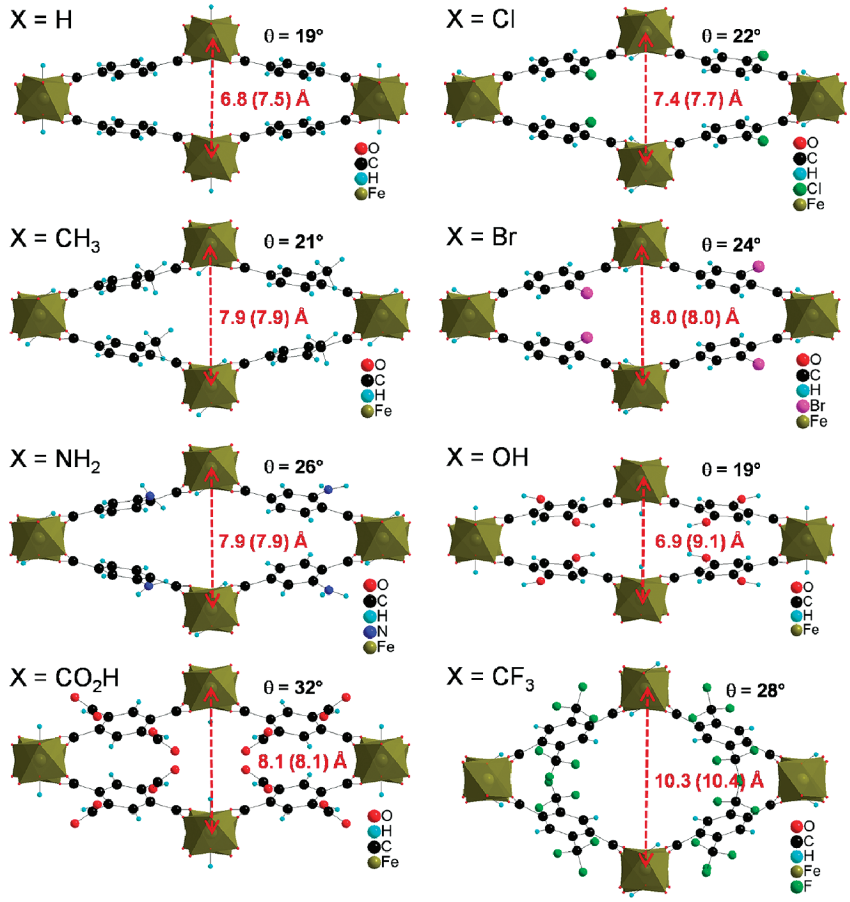

Figure 6. Projection along the Fe chain axis of the simulated crystal structures of the dry MIL-53(Fe)-X_n solids. Values of the *b* crystallographic parameter in both the dry and hydrated (parentheses) forms is given, as well as the θ angle in the dry form (see the definition in Figure 7).

O−C−O group is bound to one Fe of the chain. This means also that the θ angle between Φ and the Fe chains, which characterizes the projection of the rotation in Figure 6, differs from the γ angle between Φ and COO.

Within the functionalized frameworks, different interactions also affect the rotation of Φ. The first of them (noted **1** in Figure 7b) relates to the coupling of −X groups with the OH of the Fe−OH−Fe chains. Depending on the nature of −X, it can give

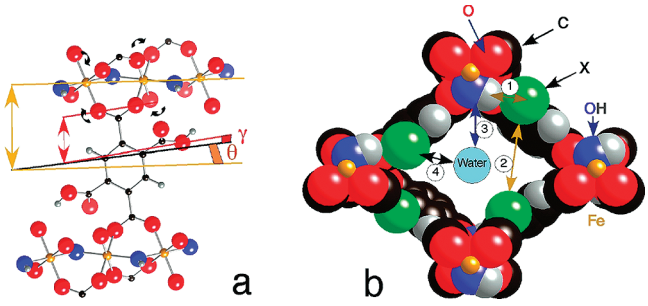

Figure 7. (a) Definition of the angles of rotation between the COO group and Φ (γ) and between the Fe−OH−Fe chains and Φ (θ); the incidence of the rotation of the COO group on the tilting of the octahedral chains is noted by black arrows. (b) Interactions occurring in the hydrated and dry forms of MIL-53(Fe)-X (the OH groups of the skeleton are in blue and gray, and the substituents X in green). Interactions **3** and **4** between water and the skeleton disappear in the dry solids in which only subsist the interactions **1** (called "inorganic−organic intraframework interaction" in the text) between X and the OH groups of the framework and **2** (called "organic−organic intraframework interaction" in the text) corresponding to the interactions between two Φ-X rings.

additional inorganic−organic intraframework hydrogen bonds (see legend of Figure 7) which will modify the position of the Φ rings. Moreover, the most stable optimized structures always come with substituting groups distributed on the opposite sides of the phenyl rings which face each other. This steric repulsion (along the *b* axis, noted **2** in Figure 7b) is the second interaction which plays a role on the orientation of the Φ rings. The final conformation is thus a complex compromise between the geometrical factors, inorganic−organic intraframework OH···X interactions, and organic−organic intraframework ΦX···ΦX steric repulsions.

To examine the potential of hydrogen bonds, the local structure of the dry forms was probed by IR, focusing on the bridging hydroxyl group (Figure 8). Different situations, depending on the nature of the functional group, are manifested.

In the absence of any interaction ν(OH) and δ(OH) bands are located at approximately 3645 and 850 cm^{-1} respectively, as in the case of MIL-53(Fe) and MIL-53(Fe)-CH_3. Their sharpness indicates a homogeneous environment. Note that a broad and weak ν(OH) band is also observed at 3300 cm^{-1} on MIL-53(Fe)-CH_3 which might be due to some impurities (this band indeed is still present when the compound is decomposed after the thermal treatment above 300 °C.) In the case of MIL-53(Fe)-$(CF_3)_2$, the ν(OH) and δ(OH) bands are situated at 3628 and 879 cm^{-1}. Such shifts are explained by the higher acidity of the Fe−OH group as shown by the adsorption of deuterated acetonitrile.[60] Spectra of the MIL-53(Fe)-Cl and MIL-53(Fe)-Br both reveal a splitting of the ν(OH) and δ(OH) bands. Considering that the hydrogen bond interaction (i) increases the δ(OH) frequency and (ii) decreases the frequency of the ν(OH) band, while the band increases in intensity and broadens, the splitting suggests the formation of a hydrogen bond with the hydroxyl group of the chains. Thus, the 3620 and 865 cm^{-1} bands on MIL-53(Fe)-Cl and the 3593 and 875 cm^{-1} bands on MIL-53(Fe)-Br are assigned to ν(OH) and δ(OH) vibrations of hydrogen bonded hydroxyl groups. The linear relation between the shift and the full width at half-maximum (fwhm) of the perturbed ν(OH) band, the main characteristics of the hydrogen bond interaction, supports this assumption (see Supporting Information for details).[61] Among the two potential hydrogen

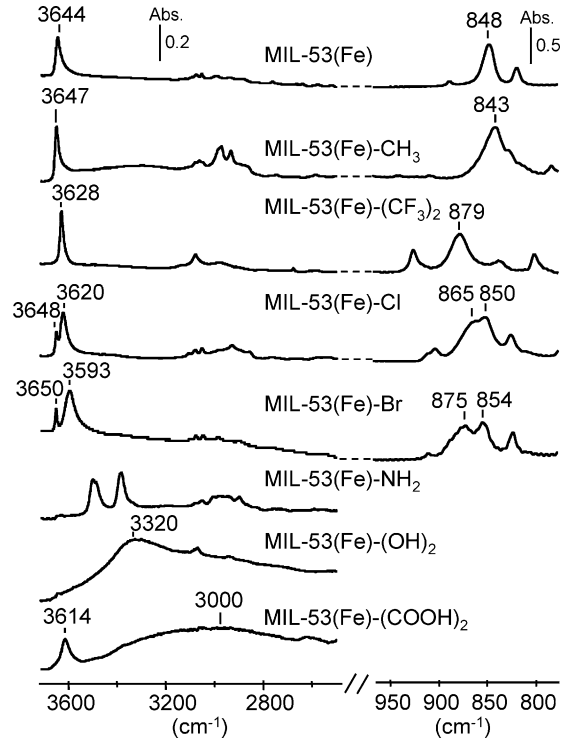

Figure 8. Infrared spectra of functionalized MIL-53(Fe)-X_n evacuated at 473 K (except for MIL-53(Fe)-$(OH)_2$, 423 K) under secondary vacuum. Left part: ν(OH) range, right part δ(OH) range (not presented for MIL-53(Fe)-NH_2, MIL-53(Fe)-$(OH)_2$, MIL-53(Fe)-$(COOH)_2$).

bond acceptors (the aromatic ring and the halogen atom), the first one can be discarded, since no interactions are observed in MIL-53(Fe) and MIL-53(Fe)-CH_3. The halogen atoms are thus involved in weak OH···X (X = Cl, Br) hydrogen bonds. This is in accordance with the short OH···X contacts deduced from the simulated structures (H···Cl = 2.52 Å, O···Cl = 3.47 Å and H···Br = 2.61 Å, O···Br = 3.57 Å).[62,63] The Fe−OH band of the MIL-53(Fe)-$(CO_2H)_2$ compound, rather broad, is situated at 3614 cm^{-1}. By analogy with results relative to Br and Cl, we assign it to the Fe−OH group in H-bonding interaction with the carboxylic group. No significant ν(OH) band appears in the spectra of MIL-53(Fe)-$(OH)_2$ and MIL-53(Fe)-NH_2 above 3550 cm^{-1} (the two sharp bands at 3491 and 3382 cm^{-1} are assigned to NH_2 stretching modes). This shows that the Fe−OH entities of both samples are H-bonded with an H-acceptor site (OH or NH_2 group respectively). In the case of MIL-53(Fe)-$(OH)_2$ and MIL-53(Fe)-$(COOH)_2$, other OH groups are present (phenolic or carboxylic). They also give rise to very broad ν(OH) bands below 3400 cm^{-1}, demonstrating that they are not free but involved in a hydrogen bonding interaction with equivalent substituent groups (or remaining water for MIL-53(Fe)-$(OH)_2$).

These intraframework interactions above can for instance explain why the unit cell volume of MIL-53(Fe)-$(CO_2H)_2$ is only slightly larger than those observed for MIL-53(Fe)-Br and MIL-53(Fe)-NH_2, whereas the functional groups are bulkier; this could be directly related to the O−H····O hydrogen bonds between the free carboxylic groups of facing linkers, which force the pores to close.[55]

(60) Vimont, A.; Clet, G., *unpublished results*.
(61) Huggins, C. M.; Pimentel, G. C. *J. Phys. Chem.* **1956**, *60*, 1615–1619.
(62) Brammer, L.; Bruton, E. A.; Sherwood, P. *Cryst. Growth Des.* **2001**, *1*, 277–290.
(63) Kovács, A.; Varga, Z. *Coord. Chem. Rev.* **2006**, *250*, 710–727.

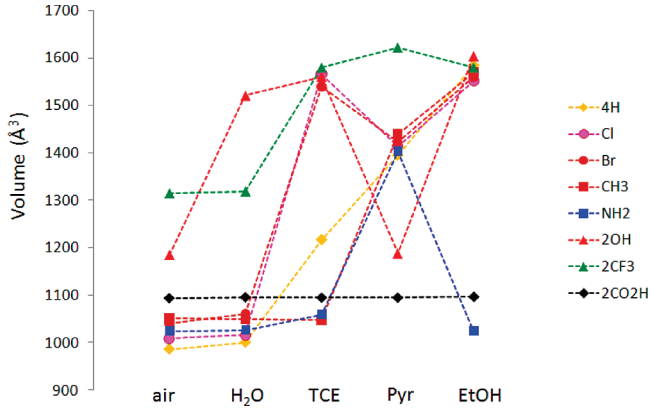

Figure 9. Unit cell volume of the MIL-53(Fe) and its modified analogues in their (air) hydrated form and immersed in various solvents. TCE, 1,1,2,2-tetrachloroethane; EtOH, ethanol; H_2O, water; Pyr, pyridine.

Among the series, both hydrated and dry MIL-53(Fe)-X solids exist in a *narrow pore* configuration. Dehydration is associated with only negligible increases or decreases of the unit cell volumes (Table S5). This suggests that the volume of the guest (water) does not play a significant role in the unit cell volume variations, at variance to the intraframework short contacts. This is in sharp contrast with our previous findings on other MIL-53(M) derivatives (M = Cr, Al, Ga), whose structures evolve from a *narrow pore* to a *large pore* form upon dehydration. Despite some previous qualitative hypotheses,[64] the reasons for this discrepancy between Fe and the other metals currently remains unfortunately unclear. Such a difference may find a possible explanation in the electronic configuration of the 3d orbitals of the various trivalent cations involved in the MIL-53-type structure. Fe^{3+}, in particular, presents a stable, symmetric half filled $3d^5$ orbital, difficult to be perturbed, whereas Cr^{3+}, for example, possesses a $3d^3$ configuration, open to host electrons from the guest molecules.

Adsorption by Immersion in Liquids. For pristine MIL-53(Fe), this discrepancy no longer exists when liquids are used instead of gases and water.[45,48] The question of whether or not the functionalization of MIL-53(Fe) can drastically change the swelling properties during the adsorption of liquids is addressed here. As already done for the nonmodified MIL-53(Fe) solid, the adsorption of liquids was performed on the hydrated (air) forms of the modified MIL-53(Fe)s rather than on the dehydrated ones. This allows starting from a homogeneous series of compounds, whereas dehydration, if not performed completely, may lead to heterogeneous results. As a consequence, this study concerns not only the adsorption of a given guest but also the *competition* between the adsorption (or coadsorption) of this given guest and water. The (air) hydrated forms of the functionalized MIL-53(Fe) solids were therefore suspended in various solvents (water, ethanol, pyridine, and 1,1,2,2-tetrachloroethane (TCE)) with variable polarity or acidity, registering drastically different XRPD patterns.

The corresponding unit-cell dimensions are reported in Table 2. The unit cell volumes for each solid/liquid pair are summarized in Figure 9 and Table S6.

One can note that MIL-53(Fe)-$(CO_2H)_2$ is an exception. It remains in its *narrow pore* form regardless of the liquid used, without any significant liquid uptake. This is probably related to the strong intraframework hydrogen bond network mentioned above, which forces the pores to remain closed.[55] Otherwise, for all the others, as already observed on the nonmodified MIL-53(Fe) solid,[48] the position of the Bragg peaks (and thus the pore opening) for a given phase strongly depends on the nature of the adsorbed liquid (Figure S10, top). Moreover, for a given liquid, the XRPD pattern depends on the nature of the functional groups (Figure S10, bottom). Unless noticed, no mixture of forms was observed in the liquid-immersed samples. As already noticed for the nonmodified MIL-53(Fe), depending on the nature of the liquid, not only the hydrated *narrow pore* and *large pore* forms but also intermediate pore openings were observed. This latter could correspond to *narrow pore* forms, whose volumes have been shown to be dependent on the steric hindrance of the guest (size and shape).[43,45]

The adsorption of ethanol leads to the *large pore* form for all the modified forms with a very similar unit cell volume within the 1550−1560 Å^3 range,[36,43,48] which corresponds to the maximum opening of the structure. In the case of MIL-53(Fe)-NH_2, this form is in equilibrium with the *narrow pore* hydrated form, which could be the consequence of strong water−framework interactions (hydrogen bonds) in the starting material, giving rise to only partial water−ethanol exchange. On the other hand, in water, most of the solids capture only a very limited amount of liquid and remain in the *narrow pore* form with unit cell volumes almost identical to those of the hydrated (air) forms, i.e. lower than 1100 Å^3 in most cases and equal to 1319 Å^3 for MIL-53(Fe)-$(CF_3)_2$ (a volume corresponding to a closed form, as seen above). A noticeable exception concerns MIL-53(Fe)-$(OH)_2$ which captures large amounts of water and exhibits the *large pore* form with a unit cell volume of 1550 Å^3, which is consistent with additional hydrogen bonds between hydroquinolic OH groups and free water molecules.

In pyridine, once again, MIL-53(Fe)-$(OH)_2$, is a special case: no adsorption occurs, and the hydrated *narrow pore* structure is maintained. For the others, a significant uptake is observed with an intermediate ($V \approx 1400$ Å^3) or complete ($V \approx 1600$ Å^3) pore opening. In the halogenated solvent (TCE), the adsorption is significant for the halogenated MIL-53(Fe) solids (−Cl, −Br, $-CF_3$) leading to the *large pore* form, whereas a few other structures, such as the apolar MIL-53(Fe)-CH_3, with similar steric hindrance, do not take any TCE and remain in the hydrated *narrow pore* form.

This part of the study shows that, in functionalized MIL-53(Fe)-X_n solids, the flexibility (and therefore the adsorption) is governed to a different extent by the host (including X)−guest interactions, and not by steric considerations. Their strength can sometimes counterbalance the intraframework interactions (which always lead to a *narrow pore* form in the original solids), allowing in this case the opening of the structures. The whole set of observations clearly proves that the selectivity for the liquid adsorption in modified MIL-53(Fe) solids depends on the solvent−host framework interaction. This conclusion suggests that, by using an adequate functionalization, an "à la carte" liquid purification/separation seems possible.

Energetics of the *np*−*lp* Transition in Modified MIL-53(Fe) Solids. The pore opening in the functionalized MIL-53(Fe) solids triggered by the adsorption of guest molecules is governed by a critical balance between the intrinsic stability of the *narrow* and *large pore* forms and the guest−framework interactions. As a preliminary step, a computational structure determination of the *large pore* forms of each functionalized MIL-53(Fe) solid was first conducted starting from the experimental unit cell parameters

(64) Liu, Y.; Her, J.-H.; Dailly, A.; Ramirez-Cuesta, A. J.; Neumann, D. A.; Brown, C. M. *J. Am. Chem. Soc.* **2008**, *130*, 11813–11818.

Table 3. Evolution of the Energy Difference between the *Large Pore (lp)* and the *Narrow Pore (np)* Forms for the Different MIL-53(Fe) Structures

Structures	$[E(lp) - E(np)]$ (kcal mol^{-1})
MIL-53(Fe)-Cl	285
MIL-53(Fe)-Br	270
MIL-53(Fe)-NH_2	230
MIL-53(Fe)-$(OH)_2$	180
MIL-53(Fe)	60
MIL-53(Fe)-CH_3	–50
MIL-53(Fe)-$(CH_3)_4$ (hypothetical)	–150
MIL-53(Fe)-$(CF_3)_2$	–170

obtained for an ethanol-containing framework (Table 2; see Supporting Information for the crystallographic data of each MIL-53(Fe)-X_n solid). These additional calculations allowed us to estimate for each functionalized form the energy difference between the lowest energetic structures obtained for the *narrow pore* and *large pore* forms. The resulting values are reported in Table 3. First, this energy difference is positive for all solids except for those substituted with $-CH_3$ and $-CF_3$ groups, which emphasizes that the most stable structure corresponds to the *narrow pore* form observed in the dry state. The lower the energy difference, the easier the MIL-53(Fe) structure will switch toward the *large pore* form in the presence of solvent molecules.

The energy cost for opening the structure thus increases in the following sequence: MIL-53(Fe)-$(CF_3)_2$ < MIL-53(Fe)-CH_3 < MIL-53(Fe) < MIL-53(Fe)-$(OH)_2$ <MIL-53(Fe)-NH_2 < MIL-53(Fe)-Br < MIL-53(Fe)-Cl. One should keep in mind that this energetic sequence is only qualitative since it has been obtained using the generic UFF force field. From the IR results, it is worth noting that the materials with a structure which is easy to open ($-CH_3$, $-(CF_3)_2$) present only free OH groups. In contrast, the most energetically stable materials in the narrow pore form ($-$Br, $-$Cl, $-(OH)_2$) present OH groups involved in inorganic−organic intraframework hydrogen bonds. This suggests that the presence of hydrogen bonded OH groups influences the *narrow pore* form stability. In these compounds, the corresponding energy barriers should be overcome by the guest−MIL-53(Fe) framework interactions when one introduces the solvent molecule. The functional groups favoring the large pore form ($-CH_3$ and $-CF_3$) only weakly interact with guests through van der Waals interactions, thus giving rise to a low energy gain through the host−guest interaction, contrarily to the groups stabilizing the narrow pore form ($-$Br, $-NH_2$, $-$OH, etc.). This is clearly illustrated by the fact that MIL-53(Fe)-CH_3 and MIL-53(Fe)-$(CF_3)_2$ do not easily open in the selected solvents (see Table 2).

Conclusion

The synthesis, on a large scale and HF-free when possible, activation, and structural analysis of a series of functionalized flexible MIL-53(Fe) hybrid solids have been reported. As expected from previous studies on the nonmodified parent MIL-53(Fe), all functional solids keep their flexible character upon adsorption/desorption, nevertheless being modulated by the presence of additional functional groups, with a complex combination of steric hindrance considerations and intraframework interactions that lead to slightly different breathing characters. Finally, the study of the adsorption of various liquids showed that the pore opening is selective and strongly depends on the guest−framework affinity, making these inexpensive and environmentally friendly nontoxic solids good candidates not only for liquid phase separation (or drug delivery) but also for gas sorption applications envisaged from the larger accessibility of the pores in their dried forms. Similar work on another series of functionalized flexible solids (MIL-88)[65] is currently under way in our laboratories.

Acknowledgment. Dr. P. L. Llewellyn and Dr. S. Bourrelly are thanked for their help in powder X-ray measurements of the activated solids, Dr. F. Dumur for his fruitful advice on linker synthesis, and Dr. S. Bauer and Prof. N. Stock for their help in the synthesis of MIL-53(Fe)-NH_2. The authors acknowledge the financial support of the French ANR 'SAFHS' (ANR-07-BLAN-0284-02), 'NOMAC' (ANR-06-CO2-008), 'CONDMOFs' (ANR-07-BLAN-1-203677) and the UE through the FP6-STREP 'DeSANNS' (SES6-020133). The ESRF is acknowledged for providing access to the Swiss-Norwegian beamline.

Supporting Information Available: Full experimental details (synthesis, characterization, XRD data, structural description, simulation methodology, cif files).

This material is available free of charge via the Internet at http://pubs.acs.org.

JA9092715

(65) Surblé, S.; Serre, C.; Mellot-Draznieks, C.; Millange, F.; Férey, G. *Chem. Commun.* **2006**, 284–286.